Available online at www.sciencedirect.com

ScienceDirect

Mendeleev Commun., 2022, **32**, 531–533

Mendeleev Communications

Photo- and ionochromic properties of new spirobenzochromene-pyranoquinoline

Anatoly V. Chernyshev,*[a] Ekaterina V. Solov'eva,[a] Irina A. Rostovtseva,[a] Nikolai A. Voloshin,[a] Oleg P. Demidov,[b] Konstantin E. Shepelenko[c] and Anatoly V. Metelitsa[a]

[a] *Institute of Physical and Organic Chemistry, Southern Federal University, 344090 Rostov-on-Don, Russian Federation. E-mail: avchernyshev@sfedu.ru*
[b] *North-Caucasus Federal University, 355035 Stavropol, Russian Federation*
[c] *Platov South-Russian State Polytechnic University, 346428 Novocherkassk, Russian Federation*

DOI: 10.1016/j.mencom.2022.07.032

A compound of the new spirobipyran-quinoline series possesses weakly pronounced photochromic properties at room temperature. Its interaction with Co^{2+}, Ni^{2+}, Zn^{2+} and Cd^{2+} ions leads to intensely colored complexes absorbing in the λ > 600 nm region, which is important for the study of biological objects. Up to three merocyanine molecules are capable of binding one metal ion, which is not typical for the previously studied indoline analogs.

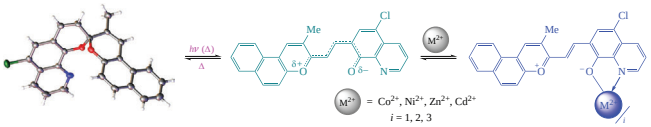

Keywords: spiropyrans, photochromism, merocyanine dyes, complex formation, NIR-dyes.

Spiropyrans belong to a widely studied class of organic photochromic compounds.[1] The transition between the colorless spirocyclic and colored merocyanine forms of spiropyrans can be induced, in addition to light, by other external stimuli such as heat,[2] medium polarity,[3] or redox potential.[4] This determines the demand for spiropyrans in the construction of a wide range of functional materials.[5] Modification of spiropyrans with chelating groups provides compounds whose photochromic reaction can modulate the formation of metal complexes.[6,7] This opens up the possibility of using spiropyrans as photo-controlled sensors of ions and molecules.[8] The increasing requirements for the spectral characteristics of such spiropyrans for biological applications stimulate the search for compounds exhibiting an optical response to metal ions in the λ > 600 nm region.[9] In this regard, synthesis and study of chelating spiropyrans with a hetarene moiety which is different from an indoline one is of high importance.

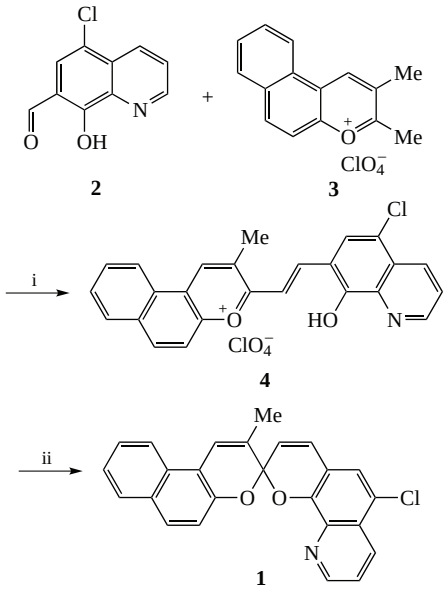

Scheme 1 *Reagents and conditions*: i, AcOH, reflux, 2 h; ii, NH_3, $CHCl_3$, room temperature.

In this study, spirobipyran (SBP) **1** was obtained by the condensation of 5-chloro-substituted hydroxyquinoline aldehyde **2** with benzo[*f*]chromenium perchlorate **3** in acidic medium and treatment of the resulting *o*-hydroxystyryl derivative with a base in chloroform (Scheme 1).

The structure of compound **1** was established by one-dimensional (^{1}H, ^{13}C) and two-dimensional (COSY ^{1}H–^{1}H, HSQC ^{1}H–^{13}C, HMBC ^{1}H–^{13}C) NMR spectroscopy, mass spectrometry and X-ray structural analysis data. The ^{1}H NMR spectrum of compound **1** (see Online Supplementary Materials, Figure S1) contains the characteristic upfield signal for the methyl group and a group of overlapped signals in the downfield region, which are related to the benzochromene and pyranoquinoline fragments. To confirm the correctness of the assignment of signals in the one-dimensional ^{1}H NMR spectrum, the two-dimensional correlation spectrum COSY ^{1}H–^{1}H was decoded (Figure S2). Assignment of signals in the one-dimensional ^{13}C NMR spectrum (Figure S3) was made using the two-dimensional correlation spectrum HSQC ^{1}H–^{13}C (Figure S4). The HMBC ^{1}H–^{13}C long-range heteronuclear correlation method was used to determine the chemical shifts of non-hydrogen carbon atoms (Figure S5).

According to the X-ray structural analysis data (Figure 1),† in the crystalline state SBP **1** exists in the spirocyclic form. The

† *Crystal data for* **1**. A light yellow crystal, $C_{25}H_{16}ClNO_2$ (*M* = 397.84), orthorhombic, space group *Pbca* (no. 61), *a* = 11.5038(3), *b* = 6.5637(2) and *c* = 49.8431(14) Å, *V* = 3763.53(18) Å^3, *Z* = 8, *T* = 100.00(10) K,

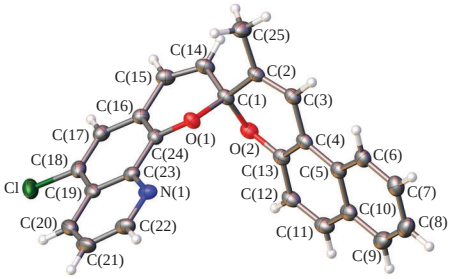

Figure 1 The molecular structure of spirobipyran **1** with atoms represented by thermal vibration ellipsoids of 50% probability.

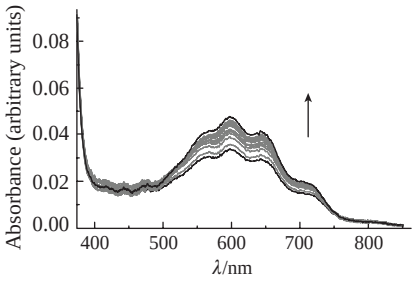

Figure 2 Absorption spectra of SBP **1** in acetone under UV light irradiation (λ = 365 nm), $C(\mathbf{1}) = 2.1 \times 10^{-4}$ M, $I^{365} = 2.2 \times 10^{-5}$ Einstein L^{-1} s^{-1}, T = 293 K, time between spectra 1 s.

carbocyclic fragments of spiropyran **1** are, except for the C(1) atom, nearly coplanar to fused pyran rings. The O(1)–C(1)–O(2) angle is close to the value characteristic of a carbon atom in the sp^3 hybrid state (107.19°). At the same time, the bond angle C(2)–C(1)–C(14) is 115.92°, which is within the deviation of the bond angles of the structurally closely related spiro compounds.[10]

An acetone solution of spirobipyran is practically colorless due to the predominance of the spirocyclic form **A** (Scheme 2). The long wavelength band of the spirocyclic form contains two maxima at 331 nm (10 500 dm^3 mol^{-1} cm^{-1}) and 346 nm (10 090 dm^3 mol^{-1} cm^{-1}) in the absorption spectrum. In the visible spectral region, a weakly intense broad structured band is observed in the region with maxima at 573, 600, 648, and 712 nm, which belongs to the colored merocyanine form **B**, which is in equilibrium with the spirocyclic form.

At room temperature, SBP **1** in acetone demonstrates positive photochromism. Irradiation of the solution with UV light (λ = 365 nm) leads to the additional coloration due to the photoinduced formation of the merocyanine form (Figure 2). The colored form lifetime is 100 s at 293 K. The low intensity of photocoloration with a sufficiently long lifetime for this class of compounds indicates a low efficiency of the photoreaction.

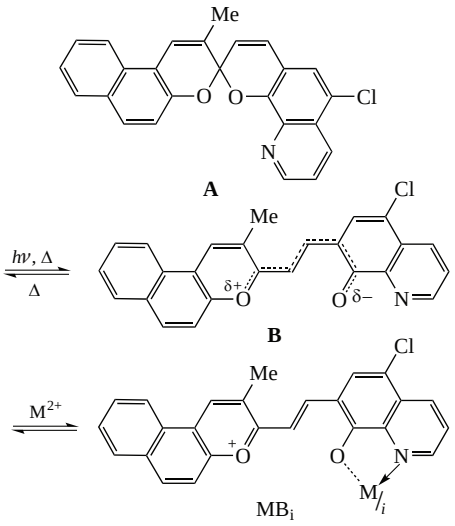

Scheme 2

The addition of Co^{2+}, Ni^{2+}, Zn^{2+} and Cd^{2+} perchlorates to an almost colorless solution of compound **1** in acetone causes the appearance of intense coloration due to the formation of complex compounds of the merocyanine form MB_i containing a chelating quinoline fragment (see Scheme 2). This was manifested in the absorption spectra by the appearance of intense bands in the visible spectral region. The significant dependence of the position, intensity, and shape of the absorption bands on the ratio of the metal and ligand concentrations appeared to be unexpected (Figure 3). To quantitatively describe the complexation equilibria, the Ostromyslensky–Job spectrophotometric method was used.[11,12] Figure 3 shows the absorption spectra of the isomolar series of SBP **1** solutions with cadmium when $C(Cd^{2+}) + C(\mathbf{1}) = 7.0 \times 10^{-5}$ M. For solutions containing a ligand excess, the absorption spectra demonstrate a broad structured band in the range of 500–800 nm with a characteristic narrow intense peak at 575 nm, as well as a weakly resolved maximum at 790 nm. The band disappears with an increase in the metal mole fraction. The dependence of the absorbance at characteristic wavelengths (575, 790 nm) on the metal mole fraction (Figure 4) indicates the formation of 1 : 3 (metal–spiropyran) complexes. At the same time, for wavelengths of 670 and 722 nm, the maximum of the diagram lies in the metal mole fraction range of 0.4–0.5, which is due to the different absorption capacities of complexes of various compositions. For Co^{2+}, Ni^{2+}, Zn^{2+} ions, the nature of the spectral changes and the isomolar diagram form are similar (Figures S7–S12). The observed spectral pattern noticeably distinguishes spirobipyran **1** from the previously described indoline analogs,[13] for which a successive increase in the metal mole fraction leads to an increase in the intensity of the long wavelength band and its slight hypsochromic shift due to the formation of 1 : 1 and 1 : 2 complexes. It should be noted that most of the spiropyrans with chelating groups described by now

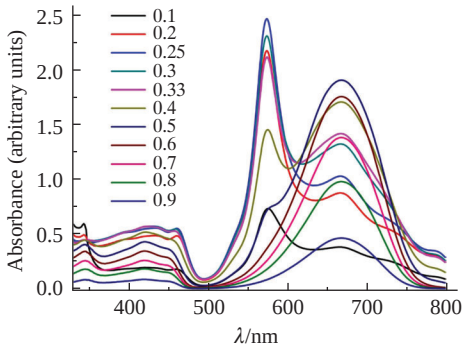

Figure 3 Absorption spectra of the isomolar series of solution **1** with cadmium, $C(Cd) + C(\mathbf{1}) = 7.0 \times 10^{-5}$ M; the numbers on a graph indicate the cadmium mole fraction.

μ(CuKα) = 1.972 mm^{-1}, d_{calc} = 1.404 g cm^{-3}, 20085 reflections measured (7.094° ⩽ 2θ ⩽ 154.032°), 3945 unique (R_{int} = 0.0534, R_{sigma} = 0.0280) which were used in all calculations. GOOF 1.104. The final R_1 was 0.0584 [$I > 2\sigma(I)$] and wR_2 was 0.1318 (all data).

The X-ray diffraction data set was recorded on an Agilent SuperNova diffractometer using a microfocus X-ray radiation source with the copper anode (CuKα, λ = 1.54184) and Atlas S2 two-dimensional CCD detector. The reflections were recorded and unit cell parameters were determined and refined using the dedicated CrysAlisPro 171.41.93a software suite.[16] The structure was solved with ShelXT program[17] and refined with ShelXL program,[18] the graphics were rendered using the Olex2 ver. 1.3.0 software suite.[19]

CCDC 2123459 contains the supplementary crystallographic data for this paper. These data can be obtained free of charge from The Cambridge Crystallographic Data Centre *via* http://www.ccdc.cam.ac.uk.

Table 1 Calculated values of effective binding constants, absorption and luminescence properties of **1**–metal complexes in acetone, T = 293 K.

M	MB_1			MB_2		MB_3	
	$\log K_1^{eff}$	λ_{max}/nm (ε/10^{-4} dm^3 mol^{-1} cm^{-1})	λ^{flu}/nm	$\log K_2^{eff}$	λ_{max}/nm (ε/10^{-4} dm^3 mol^{-1} cm^{-1})	$\log K_3^{eff}$	λ_{max}/nm (ε/10^{-4} dm^3 mol^{-1} cm^{-1})
Co	8.02 ± 0.08	672 (6.90)	–	7.17 ± 0.07	690 (9.79)	5.83 ± 0.03	582 (11.45), 683 (9.25)
Ni	8.2 ± 0.1	675 (6.64)	–	6.6 ± 0.1	709 (14.24)	6.9 ± 0.1	580 (12.19), 685 (8.88)
Zn	8.2 ± 0.1	659 (6.66)	749	7.60 ± 0.06	675 (11.88)	5.77 ± 0.03	575 (13.05), 671 (9.23), 782 (2.59)
Cd	7.27 ± 0.05	669 (6.69)	750	5.5 ± 0.1	698 (10.93)	6.37 ± 0.07	575 (17.42), 669 (6.96), 787 (2.46)

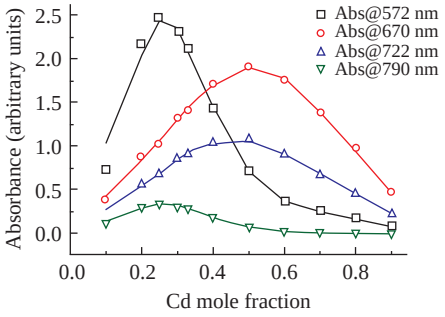

Figure 4 Continuous variation plot of **1** with cadmium at the characteristic observation wavelengths. Points are experimental data, curves are calculated values.

are characterized by 1 : 1 and 1 : 2 stoichiometry of the complexes (metal–ligand). In recent work, a rare example of a 1 : 4 (metal–ligand) complex of 8-methoxy-1′,3′,3′-trimethyl-6-nitrospiro-[chromene-2,2′-indoline] with calcium ions has been presented both in the solid phase and in solution.[14] The absorption spectra of the isomolar series for this case have not demonstrated significant changes in the visible region. On the other hand, the spectral evolution shown in Figure 3 was observed earlier for spirooxazines (structural analogs of spiropyrans) during the formation of merocyanine aggregates.[15] Under conditions reducing the solubility of merocyanine isomers, aggregates of H and J types were formed. In this case, the formation of H-aggregates was accompanied by the appearance of a narrow intense band on the short wavelength side of the merocyanine absorption band. The appearance of J-aggregates caused the appearance of a band on the long wavelength side.

To calculate the complexation constants of SBP **1**, a sequential 1 : 3 complex formation model was used (see Online Supplementary Materials and Table 1). Spirobipyran **1** forms rather stable complexes with Co^{2+}, Ni^{2+}, Zn^{2+}, Cd^{2+} ions, the stepwise formation constants of which (K_1^{eff} and K_2^{eff}) are 1–2 orders of magnitude higher than in the case of the indoline analog.[13] The complex formation at the third step is also characterized by a high constant. The absorption characteristics of 1 : 1 and 1 : 2 SBP **1** complexes are typical for merocyanine spiro-linked pyran-quinoline derivatives. Significant spectral differences revealed at the third stage of the interaction of SBP **1** merocyanine with metal salt and associated with the appearance of a narrow peak at 575 nm and a long wavelength shoulder at 780 nm, along with a wide band located in the 660–700 nm range, are probably due to the specific interaction of merocyanine ligands undergoing in the same way as in the case of H and J type aggregates formation. It should be noted that the 1 : 1 complexes with Zn^{2+} and Cd^{2+} ions exhibit low-intensity fluorescence with a maximum of 750 nm.

In conclusion, a compound of a new series of spirobipyranquinolines has been obtained. Its structure was established by NMR spectroscopy, mass spectrometry, and X-ray diffraction analysis. The compound exhibits weakly pronounced photochromic properties at ambient temperature. Interaction with Co^{2+}, Ni^{2+}, Zn^{2+} and Cd^{2+} ions results in the formation of intensely colored complexes, which absorb in the region of λ > 600 nm. Up to three merocyanine molecules can bind one metal ion. This phenomenon was not observed for the previously studied indoline analogs.

This work was financially supported by Russian Foundation for Basic Research (grant no. 20-33-70082).

Online Supplementary Materials

Supplementary data associated with this article can be found in the online version at doi: 10.1016/j.mencom.2022.07.032.

References

1 L. Kortekaas and W. R. Browne, *Chem. Soc. Rev.*, 2019, **48**, 3406.
2 J. H. Day, *Chem. Rev.*, 1963, **63**, 65.
3 W. Tian and J. Tian, *Dyes Pigm.*, 2014, **105**, 66.
4 J. F. Zhi, R. Baba, K. Hashimoto and A. Fujishima, *J. Photochem. Photobiol., A*, 1995, **92**, 91.
5 R. Klajn, *Chem. Soc. Rev.*, 2014, **43**, 148.
6 J. D. Winkler, C. M. Bowen and V. Michelet, *J. Am. Chem. Soc.*, 1998, **120**, 3237.
7 E. V. Solov'eva, N. A. Voloshin, A. V. Chernyshev, Yu. S. Reutova and A. V. Metelitsa, *Dokl. Chem.*, 2020, **494**, 141.
8 A. A. Ali, R. Kharbash and Y. Kim, *Anal. Chim. Acta*, 2020, **1110**, 199.
9 Y. Zhang, Q. Zhou, N. Tian, C. Li and X. Wang, *Inorg. Chem.*, 2017, **56**, 1865.
10 J. Harada, Y. Kawazoe and K. Ogawa, *Chem. Commun.*, 2010, **46**, 2593.
11 I. Ostromisslensky, *Ber. Dtsch. Chem. Ges.*, 1911, **44**, 268.
12 P. Job, *Ann. Chim.*, 1928, **9**, 113.
13 A. V. Chernyshev, A. V. Metelitsa, E. B. Gaeva, N. A. Voloshin, G. S. Borodkin and V. I. Minkin, *J. Phys. Org. Chem.*, 2007, **20**, 908.
14 T. J. Feuerstein, R. Müller, C. Barner-Kowollik and P. W. Roesky, *Inorg. Chem.*, 2019, **58**, 15479.
15 A. V. Metelitsa, C. Coudret, J. C. Micheau and N. A. Voloshin, *RSC Adv.*, 2014, **4**, 20974.
16 *CrysAlisPro*, *Version 171.41.93a*, Rigaku Oxford Diffraction, 2015, https://www.rigaku.com/products/crystallography/crysalis.
17 G. M. Sheldrick, *Acta Crystallogr.*, 2015, **A71**, 3.
18 G. M. Sheldrick, *Acta Crystallogr.*, 2015, **C71**, 3.
19 O. V. Dolomanov, L. J. Bourhis, R. J. Gildea, J. A. K. Howard and H. Puschmann, *J. Appl. Crystallogr.*, 2009, **42**, 339.

Received: 29th November 2021; Com. 21/6764